Available online at www.sciencedirect.com
ScienceDirect
Applied Mathematical Modelling 31 (2007) 1001–1014
APPLIED MATHEMATICAL MODELLING
www.elsevier.com/locate/apm

Simulation of free turbulent particle-laden jet using Reynolds-stress gas turbulence model

Miroslav Sijercic, Srdjan Belosevic *, Zarko Stevanovic

"Vinca" Institute of Nuclear Sciences, Laboratory for Thermal Engineering and Energy, P.O. Box 522, 11001 Belgrade, Serbia and Montenegro

Received 1 September 2004; received in revised form 1 July 2005; accepted 16 March 2006
Available online 12 June 2006

Abstract

Free two-phase flows occur in many practical applications, such as sprays or particle drying and combustion. This paper deals with mathematical modelling of a free turbulent two-phase jet. A steady, axisymmetric, dilute, monodisperse, particle-laden, turbulent jet injected into a still environment, has been considered. The model treats the gas-phase from an Eulerian standpoint and the motion of particles from a Lagrangian one. Closure of the system of time averaged transport equations has been accomplished by using a Reynolds-stress turbulence model. The particles–fluid interaction has been considered by the PSI-Cell concept. Both the effect of interphase slip and the effect of particle dispersion have been taken into account.

Results of the model have been compared with experimental data for axial and radial profiles of gas-phase mean and turbulent quantities and solid-phase mean velocity. Accuracy of model predictions of particle-laden free jet time averaged characteristics as well as turbulence correlation coefficients have been improved. The modelling of observed turbulence anisotropy levels and correlation coefficients need to be carried out with special care. The model has provided insight into the turbulence structure and aerodynamic characteristics of the particle-laden free jet.

A brief sensitivity study has been performed as well, indicating that the specification of inlet boundary conditions exerts pronounced effects on predictions. In this paper, the study refers to the effect of the turbulence kinetic energy dissipation rate, while the other inlet boundary conditions have been applied with respect to the referent measurements.

Keywords: Free particle-laden jet; Turbulence; Eulerian–Lagrangian approach; Reynolds-stress model

1. Introduction

Free two-phase jet flows are extensively used in various engineering applications, such as sprays, aerosol reactors, particle separators, particle drying and combustion. This paper deals with mathematical modelling

* Corresponding author. Tel.: +381 11 245 82 22x343; fax: +381 11 245 36 70.
E-mail address: v1belose@vin.bg.ac.yu (S. Belosevic).

0307-904X/$ - see front matter © 2006 Elsevier Inc. All rights reserved.
doi:10.1016/j.apm.2006.03.019

of two-phase round free turbulent jet and complements the experimental research of free turbulent two-phase flow [1]. These experiments have considered dilute solid-particle-laden jets in a still environment. Such jets point out the effects of particle dispersion by turbulence, while minimizing influence of particle collisions.

Problems of modelling free jets in general, arise because of the non-existence of sharp edges of the physical fields, i.e., of the calculation domain, resulting in unexpected difficulties in solution convergence. So, although more suitable for experimental investigation than enclosed flows, both single-phase and multiphase free jets proved to be much more complex for mathematical modelling.

In order to get introduced to the problem, earlier theoretical and experimental investigations of particle-laden jets have been reviewed [2]. Theoretical investigations of particle-laden jets have given a number of different models so far. For example, there are models that neglect the effects of slip between the phases and give accurate predictions only for particle sizes smaller than in most practical applications [3,4]. A different group of models, sometimes called quasilaminar models [5] take into account interphase slip, but neglect turbulent dispersion of particles, which means that only particle convective velocity is considered. Such an approximation could be appropriate only for flows containing large particles. In general, these two groups of models appear to have limited ability for modelling practical particle-laden flows. Finally, a number of models, that consider both the effect of interphase slip and the effect of particle dispersion, have been developed. One of the particle dispersion models is well known Monte-Carlo simulation, introduced by Yuu et al. [6], using random sampling for turbulent fluctuation velocity in conjunction with trajectory model for particle motion. Gosman and Ioannides [7] first have proposed a more comprehensive approach, where flow properties for the stochastic calculations are computed with a k–ε turbulence model. This approach has been a basis for a number of the particle dispersion model modifications, such as [8,9]. Comprehensive and comparative analyses of different two-phase jet models are given in [1,8] and some novel approaches and modifications in [10–16]. In addition, the significant advances on free turbulent jets Large Eddy Simulations [17] and LES-based Eulerian and Lagrangian particle-laden flow simulations [18–23], have been achieved in recent years, as well as the advances in DNS two-phase flow studies [19,22,24]. The simulations coupling Lagrangian particles tracking with LES [18,20,21,23] or DNS of the carrier-phase turbulence, or Eulerian–Eulerian DNS simulations [24] are powerful investigation tools, useful for evaluation of different modeling approaches. Still, both LES and DNS simulations are numerically very expensive for practical applications.

For gas turbulence simulation, a k-ε turbulence submodel is continuously being used in a wide range of applications, both in conjunction with Eulerian two-phase flow models [13,14] and Eulerian–Lagrangian approach [9,10]. On the other hand, although its application for single-phase free flows has showed an adequate prediction of a flat jet development, it has failed considerably when considering a round axisymmetric free jet development. It has over predicted by 40% the spreading of a round free jet [25]. Thus, it is quite logical that the k-ε turbulence model does not give good results also in the case of multiphase round turbulent free jet [26]. In this work, we have tried to find the solution on the basis of Reynolds-stress gas turbulence model, which accounts for anisotropy of flow, supposing that the main reason for obtaining undesirable results is the isotropy assumption in the k–ε turbulence model. The particles–fluid interaction has been considered by the PSI-Cell concept. Both the effect of interphase slip and the effect of particle dispersion have been taken into account. A stochastic approach to particle dispersion such as the Monte-Carlo method has the problem of simplicity of the simulated turbulence field. In this work, we have chosen one derivative of a phenomenological model, mainly because it is much closer to the physical essence of the problem. A gradient diffusion approach has been used, introducing the particle diffusion velocity.

2. Mathematical model

2.1. Gas-phase mathematical model

In order to overcome some uncertainties in calculation of the free two-phase jet, in this paper, we have analyzed some specific approaches to solve this problem: (a) anisotropy of turbulent components is introduced; (b) the boundary region of the jet and the surrounding stationary fluid has been implicitly treated in the calculations; (c) boundary conditions, that are set in quiescent fluid, have been described based on the known pressure in the fluid surrounding the jet.

The mean velocity field of the gas-phase of the two-phase free flow may be described by the system of equations derived from Reynolds equations for stationary turbulent flow:

$$\begin{aligned}\frac{\partial}{\partial x_j}(\rho U_i U_j) &= -\frac{\partial P}{\partial x_i} + \frac{\partial}{\partial x_j}\left[\mu\frac{\partial U_i}{\partial x_j} - \rho\overline{u_i' u_j'}\right] + S_{\mathrm{p}}^{U_i} \\ \frac{\partial(\rho U)}{\partial x_i} &= 0,\end{aligned} \tag{1}$$

where $S_{\mathrm{p}}^{U_i}$ describes influence of particulate phase on gas-phase. In Eq. (1), U_i and u_i' are components of mean velocity and fluctuating velocity, respectively; P is mean static pressure, ρ is density, μ is dynamic viscosity and x_i, x_j are coordinates in general notation.

The additional source terms $S_{\mathrm{p}}^{u_i}$ represent the sum of momentum change of all particles, which cross the control volume, during their residence time in the considered control volume. General form of this term for x-axis is:

$$S_{\mathrm{p}}^{u} = \Delta M_{\mathrm{p}}^{x} = \frac{1}{V}\frac{\pi}{6}\rho_{\mathrm{p}}\Sigma_i\Sigma_j\left[\left(u_{\mathrm{p},ij}d_{\mathrm{p},ij}^3\right)_{\mathrm{in}} - \left(u_{\mathrm{p},ij}d_{\mathrm{p},ij}^3\right)_{\mathrm{out}}\right]\dot{N}_{ij}, \tag{2}$$

where u_{p} is instantaneous particle velocity, d_{p} particle diameter, V is volume, $\dot{N}_{i,j}$ is particle number flow rate (for particles starting location 'i' and initial particle diameter class 'j'). Note that subscript 'p' refers to particles.

Mathematical modeling of the continuous phase has been based on models developed for single-phase flows, but with the corrections due to the presence of particles.

Closure of the system of Reynolds averaged equations of momentum and continuity for stationary turbulent flow of incompressible fluid has been carried out based on the solution of equations for turbulent stress, having the exact form:

$$\begin{aligned}U_k\frac{\overline{\partial u_i' u_j'}}{\partial x_k} = &-\left[\overline{u_j' u_k'}\frac{\partial U_i}{\partial x_k} + \overline{u_i' u_k'}\frac{\partial U_j}{\partial x_k}\right] + \frac{\partial}{\partial x_k}\left(\nu\frac{\overline{\partial u_i' u_j'}}{\partial x_k}\right) - \left[2\nu\overline{\left(\frac{\partial u_i'}{\partial x_k}\right)\left(\frac{\partial u_j'}{\partial x_k}\right)}\right] + \left[\overline{\frac{p'}{\rho}\left(\frac{\partial u_i'}{\partial x_j} + \frac{\partial u_j'}{\partial x_i}\right)}\right] \\ &- \frac{\partial}{\partial x_k}\left[\overline{u_i' u_j' u_k'} + \overline{\frac{p'}{\rho}\left(\delta_{\mathrm{jk}}u_i' + \delta_{ik}u_j'\right)}\right],\end{aligned} \tag{3}$$

(where ν is kinematic viscosity, p' is pressure fluctuation and $\overline{u_i' u_j'}, \overline{u_i' u_k'}, \overline{u_j' u_k'}$ refer to the components of Reynolds stresses), or: $C_{ij} = G_{ij} + T_{ij} + E_{ij} + \Phi_{ij} + D_{ij}$.

Convective transport (C_{ij}), production due to main flow deformations (G_{ij}), and viscous diffusion (T_{ij}), may be used in their exact form. For modelling of the other terms, approximations based on the model described in [27] have been chosen. Redistribution between components of stress (interactions of pressure and flow deformations) is given as:

$$\Phi_{ij} = -c_1\frac{\varepsilon}{k}\left(\overline{u_i' u_j'} - \frac{2}{3}\delta_{ij}k\right) - \alpha\left(G_{ij} - \frac{2}{3}\delta_{ij}G\right) - \beta\left(D_{ij} - \frac{2}{3}\delta_{ij}G\right) - \gamma k\left(\frac{\partial U_i}{\partial x_j} + \frac{\partial U_j}{\partial x_j}\right), \tag{4}$$

where $k = \overline{u_k' u_k'}/2$ is kinetic energy of turbulence, $G = G_{kk}/2$ is production of turbulent kinetic energy, δ_{ij} is Kronecker delta, while:

$$\begin{aligned}G_{ij} &= -\left(\overline{u_i' u_k'}\frac{\partial U_j}{\partial x_k} + \overline{u_j' u_k'}\frac{\partial U_i}{\partial x_k}\right), \\ D_{ij} &= -\left(\overline{u_i' u_k'}\frac{\partial U_k}{\partial x_j} + \overline{u_j' u_k'}\frac{\partial U_k}{\partial x_i}\right).\end{aligned} \tag{5}$$

Coefficients α, β and γ are mutually dependent and are determined by coefficient c_2: $\alpha = (8 + c_2)/11$; $\beta = (8c_2 - 2)/11$; $\gamma = (30c_2 - 2)/55$. Viscous destruction is described by the dissipation of turbulent kinetic energy ε, ($E_{ij} = -(2/3)\varepsilon$), for which the transport equation is solved:

$$U_j \frac{\partial \varepsilon}{\partial x_j} = \frac{\partial}{\partial x_i}\left[\left(\nu + C_\varepsilon \frac{k}{\varepsilon}\overline{u_i' u_j'}\right)\frac{\partial \varepsilon}{\partial x_j}\right] + C_{\varepsilon 1} G \frac{\varepsilon}{k} - C_{\varepsilon 2}\frac{\varepsilon^2}{k}. \tag{6}$$

Diffusion transport of turbulent stress components is modeled by the expression:

$$D_{ij} = c_s \frac{\partial}{\partial x_k}\left(\frac{k}{\varepsilon}\overline{u_k' u_\ell'}\frac{\partial \overline{u_i' u_j'}}{\partial x_\ell}\right). \tag{7}$$

The resulting model has six constants, with values based on the recommendations from the literature, experimental data and numerical optimization:

c_1	c_2	c_s	$C_{\varepsilon 1}$	$C_{\varepsilon 2}$	C_ε
1.5	0.4	0.22	1.45	1.9	0.15

Turbulence modulation due to presence of particles is not considered. This is not a limitation of the approach we have chosen, because the effects of turbulence modulation are small for dilute particle-laden flows examined here. In [13], for a dilute particle-laden round jet, gas-phase Reynolds stresses have been calculated according to an algebraic stress model in connection with a standard k-ε model, but without interaction terms due to the particles-estimated to have small influence compared to the other terms. The Reynolds-stress gas-turbulence model extended in order to account for the effects of turbulence modulation, is presented in [12], for the case of axisymmetric, confined, particle-laden jet.

2.2. Particle motion and diffusion

For the dispersed phase, it is possible to use either Eulerian or Lagrangian approach. A Lagrangian approach is closer to the physical reality and gives more information (trajectories, particle residence time in considered control volume, etc.) necessary for more accurate prediction of particle motion in the turbulent field.

Motion of individual particles in a Lagrangian field is described by the Basset equation, formulated for turbulent flow by Hinze [28].

In most cases the pressure forces, forces due to the particle "added" mass, Basset and Magnus forces may be neglected. Instantaneous equation of motion for an individual particle is thus reduced to:

$$m_\mathrm{p}\frac{\mathrm{d}\vec{u}_\mathrm{p}}{\mathrm{d}\tau} = \frac{1}{2}C_\mathrm{D}\rho A_\mathrm{p}|\vec{u}-\vec{u}_\mathrm{p}|(\vec{u}-\vec{u}_\mathrm{p}) + \frac{d_\mathrm{p}^3\pi}{6}(\rho_\mathrm{p}-\rho)\vec{g}, \tag{8}$$

where m_p is particle mass, A_p is particle cross-section area, $C_\mathrm{D} = (24/Re_\mathrm{p})(1+0.15Re_\mathrm{p}^{0.67})$ is the drag coefficient of relative particle motion, and $Re_\mathrm{p} = d_\mathrm{p}|\vec{u}-\vec{u}_\mathrm{p}|/\nu$ is the Reynolds number of relative motion. Vectors $\vec{u}, \vec{u}_\mathrm{p}, \vec{g}$ are gas velocity, particle velocity and gravitational acceleration, respectively.

Introducing the coefficient of particle diffusivity $\gamma = \Gamma_\mathrm{d} + \Gamma_\mathrm{d}' = \frac{1}{2}C_\mathrm{D}\rho A_\mathrm{p}|\vec{u}-\vec{u}_\mathrm{p}|$ in Eq. (8) and applying the time-averaging procedure yields:

$$m_\mathrm{p}\frac{\mathrm{d}\vec{U}_\mathrm{p}}{\mathrm{d}\tau} = \Gamma_\mathrm{d}(\vec{U}-\vec{U}_\mathrm{p}) + \overline{\Gamma_\mathrm{d}', (\vec{u}-\vec{u}_\mathrm{p})} + \frac{d^3\pi}{6}(\rho_\mathrm{p}-\rho)\vec{g}. \tag{9}$$

Second term on the right-hand side of Eq. (9) is the consequence of the turbulent fluctuations in the flow. Its determination presents a problem not yet fully clarified. One possible approach may be to separate particle velocity into convective and diffusion parts:

$$\vec{U}_\mathrm{p} = \vec{U}_\mathrm{pc} + \vec{U}_\mathrm{pd}. \tag{10}$$

Convective particle velocity can be obtained by solving the equation of particle motion in quasilaminar fluid flow. In Lagrangian field, equations of particle motion are integrated along trajectories with a constant particle number flow rate. Particle motion, as well as the turbulence itself, is essentially three-dimensional. Regardless of the fact that for an axisymmetric problem the tangential component of the mean velocity is zero,

there are particle oscillations with fluctuation velocity w'_p in the tangential direction, resulting in a centrifugal force. Axial and radial components of convective particle velocity are thus obtained from the following equations:

$$\begin{aligned} m_p \frac{dU_{pc}}{d\tau} &= C_{D,x}\rho|U - U_{pc}|(U - U_{pc})\frac{A_p}{2} + \frac{d_p^3\pi}{6}(\rho_p - \rho)g \\ m_p \frac{dV_{pc}}{d\tau} &= C_{d,r}\rho|V - V_{pc}|(V - V_{pc})\frac{A_p}{2} + m_p\frac{\overline{w_p'^2}}{r} \end{aligned} \tag{11}$$

Expression for diffusion particle velocity should take into account that turbulence has less influence on larger than on smaller particles, and that this influence depends on the turbulence intensity. These influences could be taken into account through the characteristic response times for particles and the fluid turbulence. Characteristic particle response time to the fluid fluctuations may be considered as approximately equal to the relaxation time:

$$\tau_p = \frac{d_p^2\rho_p}{18\ \mu}. \tag{12}$$

Turbulence characteristic time is Lagrangian integral turbulent time scale:

$$\tau_t = \frac{\ell_E}{\left(\overline{u'^2}\right)^{0.5}} = \frac{v_t}{\overline{u'^2}}, \tag{13}$$

where ℓ_E is Eulerian integral length scale of turbulence and u' gas velocity turbulent fluctuation.

For determining the particle turbulent diffusion, analogy with the turbulent diffusion of the continuous phase has been sought for. Following preposition of Melville and Bray [29], one can come to expression:

$$v_p^t = v_t(1 + \tau_p/\tau_t)^{-1}, \text{ where } v_t = C_\mu\rho\frac{k^2}{\varepsilon}, \tag{14}$$

where v_t and v_p^t are turbulent diffusivity of gas and particles, respectively and C_μ is constant (known from k-ε turbulence model).

Particle dispersion by diffusion velocity is highly stochastic process. Sufficiently large particle number density in the fluid, points to the possibility of reducing the problem to the global, averaged effect. Thus, we come to an assumption [30], that a particle diffusion flux can be expressed in the same way as diffusive transport of scalar variables, and may be connected to the mass transport relative to the main flow:

$$\vec{J}_p = -\Gamma_p\nabla\rho_{p,c} = (\vec{U}_p - \vec{U}_{pc})\rho_{p,c} = \vec{U}_{pd}\rho_{p,c}, \tag{15}$$

where $\rho_{p,c}$ is the particle cloud bulk density. Diffusion velocity is thus obtained from the relation:

$$U_{pd} = -\frac{1}{N_p}\Gamma_p\nabla N_p, \tag{16}$$

where $\Gamma_p = v_p^t/\sigma_p$ is the coefficient of turbulent particle diffusivity and N_p ($1/m^3$) is the particle number density (particle concentration), being constant along each particle trajectory considered, even in the case of interphase mass exchange.

To determine diffusion velocity of particles in two-phase flow, Eq. (16), it is also necessary to know the particles concentration field. It is possible to obtain particle concentration from Lagrangian particle tracking, as done in the paper. In the stationary conditions, when the flow rate of particles entering the finite volume cell is equal to the outflow rate of the particles, local values of particle concentrations can be approximated on the basis of the number of particles entering the finite volume:

$$N_p = \sum_i \sum_j \frac{\dot{N}_{ij}}{A_{in}U_{p,ij}}, \tag{17}$$

where A_{in} is the finite volume inlet cross-section area (equal to the outlet cross-section area). Local Eulerian velocities of the dispersed phase are determined as the mean values of velocities at all trajectories crossing the exit boundary of the scalar cell and at the point of that crossing:

$$U_p = \frac{\Sigma_i \Sigma_j U_{p,ij} \dot{N}_{ij}}{\Sigma_i \Sigma_j \dot{N}_{ij}}, \quad \dot{N}_{ij} = \frac{6 Z_i Z_j \dot{m}_p}{\pi \rho_p d_{pj0}^3}, \tag{18}$$

where $\dot{N}_{ij}$ (1/s) is particle number flow rate, from starting location 'i' (with mass fraction Z_i) and initial particle diameter class d_{pj0} (with mass fraction Z_j), ρ_p is a density of individual particle, while $\dot{m}_p$ is the particles mass flow rate.

2.3. Boundary and initial conditions

2.3.1. Gas-phase

Special attention has been paid to the boundary conditions, which should be posed in the "quiescent" fluid. Values of velocity components perpendicular to these free boundaries have been determined from the known pressure on these boundaries (which is also equal to that in the quiescent fluid) [28]. This was described in our earlier works, for example [31].

For these free boundaries, which separate the flow field from its surroundings, it is possible to fix the zero values of the variables, or values of their derivatives, or to extrapolate the values of the variables in the vicinity of the boundary. These possibilities have also been used for other variables in this paper.

Velocity components parallel to the outlet boundary have been determined based on the condition of negligible changes ($\partial V/\partial r = 0$, where V is mean radial velocity and r is coordinate in radial direction). Values for other variables at the outlet boundary have been determined, considering the non-uniformity of the grid, by extrapolating the upstream values. The inlet profiles of the variables have been determined by the nature of the problem. The nozzle wall in the plane of the inlet cross-section has been described by the standard wall functions. For the axisymmetric flow, radial velocity and radial gradients of all variables at the axis are zero.

2.3.2. Dispersed phase

The general form of the equation of the dispersed phase in Lagrangian field is:

$$\mathrm{d}\xi/\mathrm{d}\tau = A - B\xi, \tag{19}$$

(for ξ—coordinate of particle in Lagrangian field) with the recurrent solution $\xi_{n+1} = \xi_n \ \mathrm{e}^{-B\Delta\tau} + A/B\ (1 - \mathrm{e}^{-B\Delta\tau})$, with constants A and B and with the initial conditions defined by the solution from the preceding time interval $\Delta\tau$. The condition of axial symmetry implies that the particles have an elastic reflection from the axis of symmetry. This means that each trajectory crossing the axis of symmetry corresponds to the other particle trajectory crossing the axis from the opposite direction. The lateral boundaries of the flow region are far from the jet boundary so the particles do not reach them, leaving the flow domain through the outlet cross-section of the jet.

2.4. Numerical details of the simulations

Discretization of partial differential equations into the system of algebraic equations was performed by means of the control volume method and hybrid numerical scheme, while the system was solved using TDMA (three-diagonal matrix algorithm). A staggered numerical grid was selected and used, because the calculations with the collocated grid did not provide a good convergence of numerical solutions. In the calculation domain (the half of the entire flow domain) structured grid with $200 \times 65 = 13{,}000$ grid nodes was used and 300 particle trajectories were numerically tracked. The grid was spreading downwards in axial direction and also from the axis of symmetry in radial direction. For the purpose of testing the consistency of the numerical results a grid refinement study was carried out and the influence of the number of the particle trajectories was examined as well. It was found that neither the application of finer numerical grids nor the further increase of the trajectories number gave any important difference in numerical results. The number of the particle trajectories

needed is more significant factor when using the stochastic models of particle dispersion than in the case of using the particle dispersion model proposed and described in the paper.

3. Modelling results and discussion

3.1. Referent experimental data

In order to evaluate the applied mathematical model and numerical procedure, we have compared obtained results for particle time averaged velocity, as well as gas-phase time averaged velocity and turbulence characteristics, to the experimental results provided by Shuen et al. [1].

The referent data [1] were obtained using a jet tube with internal diameter of 10.9 mm and the particle-laden jet was directed vertically downward within the test cage into a room of still air. The initial conditions of both phases were measured at the jet exit, i.e., at $x/d = 1$, where 'x' is coordinate in axial direction and 'd' is injector diameter.

In the paper, we have compared our numerical results with referent experimental data for one size of sand particles, i.e., for Sauter mean diameter 79 μm and for 'loading ratio' (ratio of injected particle mass flow rate to air flow rate) of 0.20, which is the case of the smallest particles and the lowest 'loading ratio' considered in measurements. It should be noted that the consideration of relatively small particles might emphasize the importance and validity of particle dispersion model applied.

Mean and fluctuating gas velocities were measured with a single-channel, frequency-shifted He–Ne laser-Doppler anemometer. Both the jet and the surroundings were seeded (0.2 μm aluminum oxide particles) to eliminate concentration bias. The tangential component of velocity fluctuations, $\left(\overline{w'^2}\right)^{1/2}$, was not measured and was assumed to be equal to $\left(\overline{v'^2}\right)^{1/2}$ when calculating the turbulence kinetic energy.

Mean and the fluctuating particle velocities were measured using the same laser-Doppler anemometer, but with no seeding particles and with low detector gain so that only strong scattering signals from test particles were observed. Mean particle velocities along the jet centerline were checked using the double-flash photographic technique.

Uncertainties in mean and fluctuating gas velocities were estimated to be less than 10% and were repeatable within 5%, while for particle velocities were less than 15%.

Detailed description of experimental installation and measuring technique is presented in [1,8] and full details and a tabulation of all experimental data are provided by Shuen et al. in [1].

3.2. Axial variation of flow properties

Predicted and measured profiles of centerline particle-laden jet flow characteristics along the axis are illustrated in Fig. 1.

Results are given for mean (time averaged) gas-phase and particle velocity and for gas turbulence intensity in axial and radial direction, all with respect to a relative axial distance x/d, where 'd' is injector diameter. Mean velocities are normalized by the values at the injector exit (inlet flow conditions) and turbulent values by a gas-phase centerline mean velocity at the axial distance considered.

In general, all predicted profiles agree fairly well with measurements. The agreement for centerline mean gas-phase velocity is practically complete, which is very important as a good basis for the rest of calculations, especially because both axial and radial profiles of gas-phase properties are given normalized by means of this velocity. The model predictions for mean particle velocities along the jet axis are in good agreement with measurements. Some differences, for $x/d = 5$ and 10, are probably the consequence of measuring uncertainties.

The axial variation of gas-phase turbulence intensities in both axial and radial direction show fairly good agreement of model with measurements, except in the near injector region, where the model underestimates turbulence levels. It should be noted that turbulence is still developing in this region, so perhaps some difficulties in modelling could be expected, regardless of the type of model applied. This underestimation was clearly showed also in [1], with the application of model which neglects the effects of slip between the phases and the model considering the effect of interphase slip, as well as the effect of particle dispersion, both using

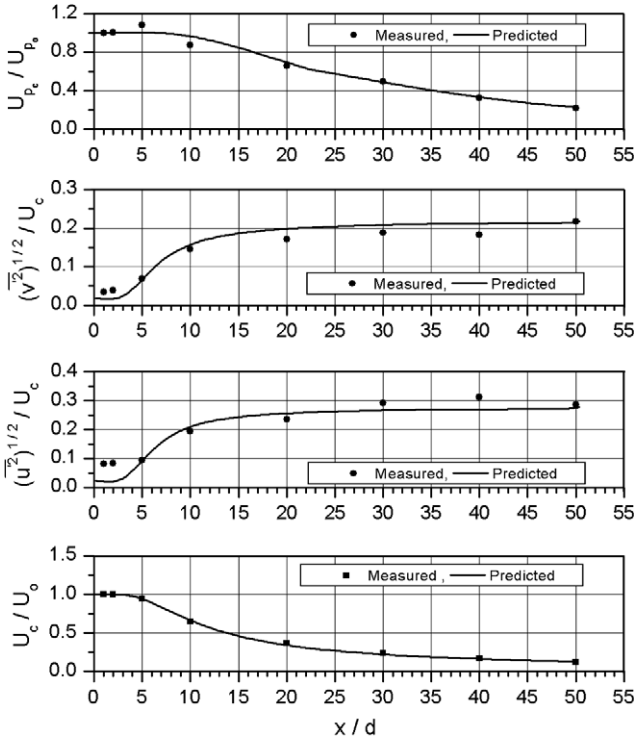

Fig. 1. Axial variation of centerline particle-laden jet flow properties.

k–ε turbulence model. It is the fact that turbulence levels at axial distances approaching $x/d = 40$, correspond to the values predicted by our model, as well as by the models used in [1], all neglecting the effects of turbulence modulation.

3.3. Radial variation of flow properties

Calculated and measured values of gas-phase properties: mean velocity, turbulence intensities in axial and radial direction and shear turbulent stress, are presented in Fig. 2 (for relative axial distance $x/d = 20$) and in Fig. 3 (for relative axial distance $x/d = 40$). For the case of low loading ratio considered, gas-phase profiles approach the single-phase jet properties.

Predictions are in good agreement with the measurements for $x/d = 20$. Prediction for mean gas-phase velocity is good for $x/d = 40$, while the agreement between predicted and measured gas-phase turbulence quantities at this axial distance is less satisfactory. The calculated radial profiles are generally too wide compared to experimental results and there is a certain overprediction. On the other hand, slightly under- and over-estimation of turbulence intensities in axial and radial direction, respectively, in the near injection region (Figs. 2 and 3) actually seems to be the sign of some measuring errors in the region.

Radial profiles of particle mean velocity are given in Fig. 4 (at $x/d = 20$) and Fig. 5 (at $x/d = 40$). Velocities are normalized by particle centerline velocity.

Predicted curves generally follow the character of change of measured values. But there are some discrepancies, probably due to the influence of gravitational force, since the particle-laden jet has been directed vertically downwards. Since the particle velocity from Figs. 4 and 5 is the particle velocity in Eulerian field, Eq. (18), which includes the influence of both particle convective and diffusion velocity, perhaps some changes in defining the particle diffusion velocity are required, in order to improve the model of particle motion and dispersion.

The predicted values of gas-phase centerline mean velocity and particle centerline velocity are $U_c = 8.808$ m/s, $U_{Pc} = 16.78$ m/s, at the axial distance $x/d = 20$ and $U_c = 4.216$ m/s, $U_{Pc} = 8.047$ m/s at the

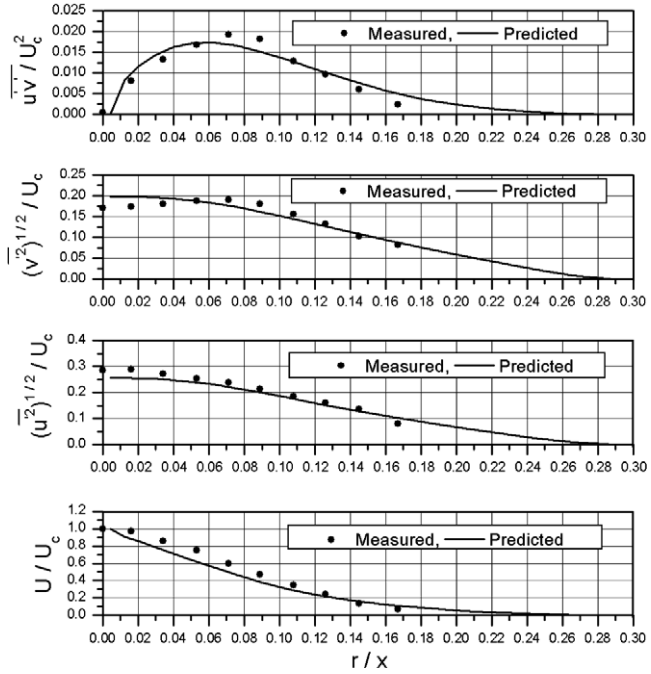

Fig. 2. Radial variation of gas-phase mean and turbulent quantities for particle-laden jet at $x/d = 20$.

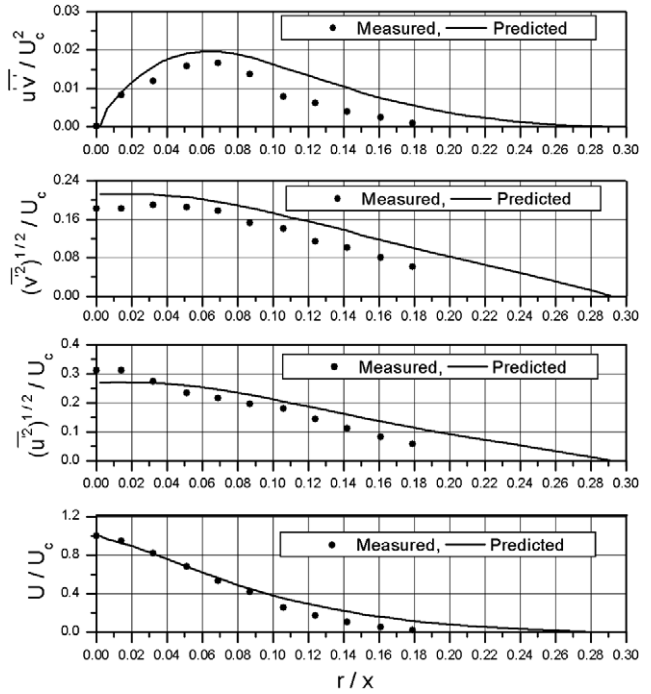

Fig. 3. Radial variation of gas-phase mean and turbulent quantities for particle-laden jet at $x/d = 40$.

axial distance $x/d = 40$. At the very beginning of the particle-laden jet U_{Pc} (=24.13 m/s) is slightly smaller than U_c (=26.07 m/s), while from the distance $x/d = 5.4$ downwards, particle centerline velocity becomes greater than the gas-phase velocity.

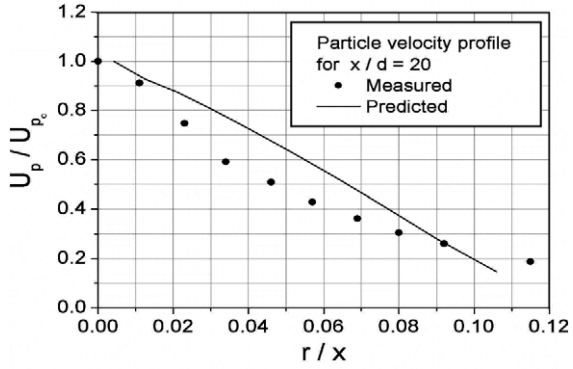

Fig. 4. Radial variation of solid-phase mean velocity at $x/d = 20$.

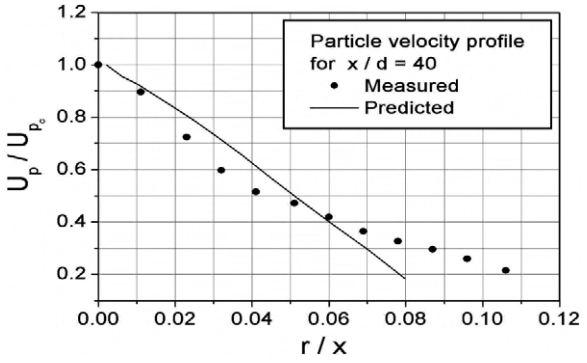

Fig. 5. Radial variation of solid-phase mean velocity at $x/d = 40$.

3.4. Gas-phase mean velocity field and turbulence field, for free particle-laden jet

The predictions for the gas-phase mean velocity vectors and contours of the velocity components are presented in Fig. 6. The velocity vector field is simple, but gives a realistic picture of flow, including entrainment of surrounding fluid. The contours of axial and radial velocity components show the spreading of the jet.

The predicted contours of the gas-phase turbulence intensities and shear turbulent stress are given in Fig. 7. The boundary of the turbulent field, irregular in shape, is clearly visible in the contours. As expected, the boundary region flow is not continuous but becomes more and more intermittent toward the outside. Fig. 7 clearly shows a feature of free turbulent flows – the intermittent character of the turbulent flow in the boundary regions between the mixing zone and the undisturbed free stream outside. Particularly in the intermittent boundary regions, the solutions of differential equations, based on the assumption of isotropy of eddy diffusion, fail. Actually, the effective value of eddy diffusion coefficient decreases rapidly in these regions as the outer edge is approached; this is reasonable, because gradient-type diffusion at a point can occur only during the period in which the flow at that point is turbulent. Reynolds stress model, used in this paper, is to overcome also this difficulty.

In addition, the calculations with no turbulent dispersion terms, i.e., with zero particle diffusion velocity, were performed. Since our calculations were done for the case of the lowest 'loading ratio' considered in referent measurements, the obtained differences for gas-phase mean and fluctuating velocities were not significant and could have not been clearly seen on diagrams or contour plots. Though, slightly lower values of gas-phase centerline mean velocity were predicted, in comparison with the basic case with particle diffusion velocity. When considering gas-phase centerline fluctuating velocities in both axial and radial direction, slightly higher values were obtained, except at the end of the jet, where the values were lower, compared with the basic case.

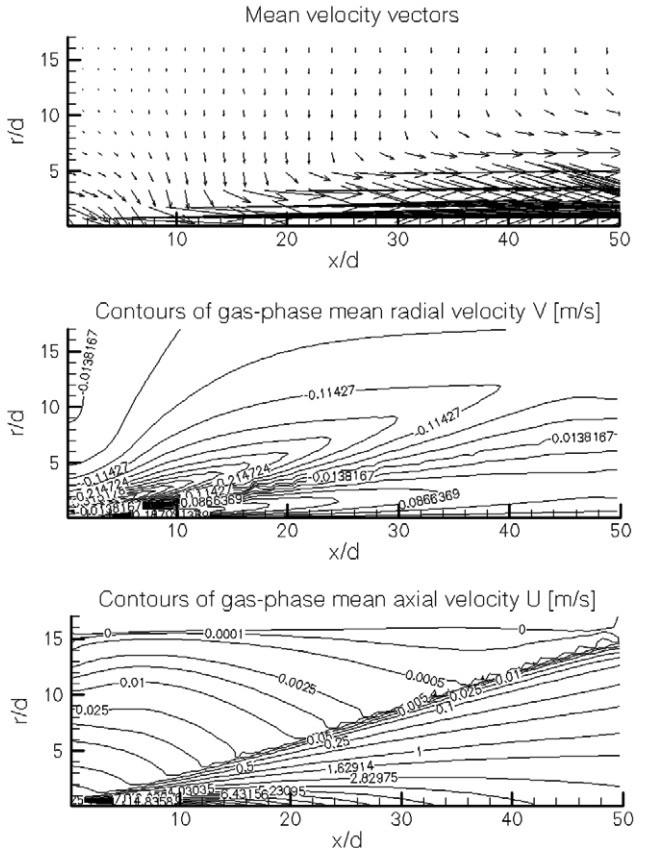

Fig. 6. Gas-phase mean velocity vectors and velocity components contours.

3.5. Sensitivity study

The results of our predictions, as well as the referent measurements [1], are sensitive to inlet boundary conditions. For the calculations in the paper, the measured values for gas-phase mean and fluctuating velocities have been used. Injector exit centerline velocities (measured and averaged at the cross-section) are: for air 26.07 m/s and for particles 24.13 m/s. All the gas-phase measurements results, except near the jet edge, are similar to the properties of the fully developed pipe flow. The inlet boundary conditions for the particle-laden jet considered are given in [1], in the form of radial profiles plots of both gas-phase and solid-phase mean and turbulent quantities (the profiles of gas-phase mean velocities, turbulence kinetic energy and Reynolds stresses and the profiles of mean particle mass flux, mean and fluctuating particle velocities and particle turbulence kinetic energy).

With respect to the fact that the calculations were performed with these measured values, only the inlet boundary conditions for dissipation rate should have been determined numerically, as a function of measured quantities. This was done in accordance with the fact that the experimental flow configuration ensured fully developed turbulent profiles at the tube exit, which formed the inlet to the free-jet flow. Non-dimensional turbulent kinetic energy dissipation rate has been described by the well-known expression for fully developed turbulent profile $\varepsilon^+ = \varepsilon R/U_\tau^3$, where U_τ is the friction velocity and R is the pipe radius. With the known turbulence kinetic energy k, the dissipation rate in the node next to the wall is given as $\varepsilon = C_\mu^{0.75} k^{1.5}/(\kappa y)$, where C_μ is structural parameter of turbulence and κ is Von Karman's constant. This approach usually gives good results if it is used for describing inflow boundary conditions and it has been here applied to the calculations of the jet. It was found that the level of dissipation rate had a very important influence on numerical results. Increase of the dissipation rate level gave the better approximation of the experimental data (we changed

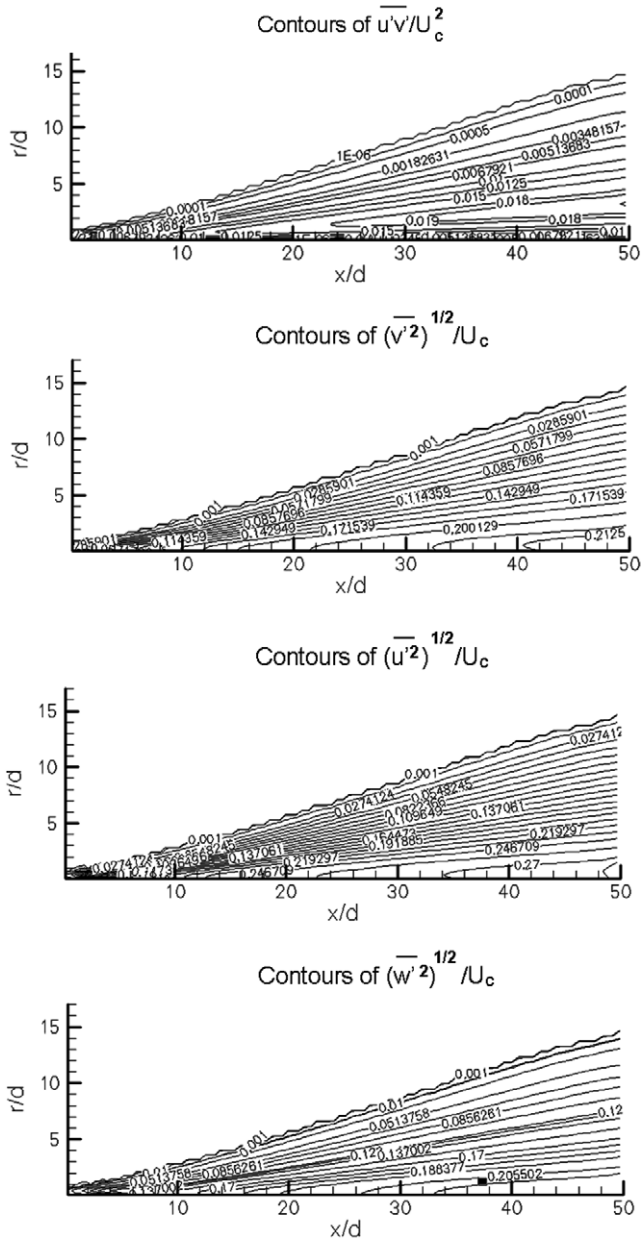

Fig. 7. Contours of the gas-phase turbulent quantities.

the dissipation rate up to 20–30%), but in our final calculations we kept the level of the dissipation rate close to the theoretical values.

4. Conclusions

The main aim of investigations described and analyzed in the paper was to develop and evaluate a mathematical model, describing a behavior of dilute particle-laden round free jet. The model takes into account both the effect of interphase slip and particle dispersion and incorporates a Reynolds-stress turbulence model, reasonably considered to be physically more appropriate than k-ε model, used in most predictions, but not

giving good results in the case of single-phase as well as multiphase round free jet. Because of the fact that the two-phase flow considered is dilute, exclusion of turbulence modulation from the model has not given significant error. This is one of a few attempts made so far, for solving this, numerically difficult problem, by means of a complex approach, including a Reynolds-stress turbulence model.

Comparisons between the results obtained using the suggested model and the results of corresponding experimental investigations made previously and taken from references, have showed mostly a good agreement and have emphasized the need for improving the model in some aspects, for example with respect to the particle dispersion. The predicted contours of gas-phase mean velocity and turbulent quantities, for particle-laden jet, are presented as well, providing the insight into aerodynamic and turbulence characteristics of the jet.

Sensitivity analyses indicate that the specification of inlet boundary conditions exerts pronounced effects on predictions. The sensitivity study in the paper refers to the effect of the turbulence kinetic energy dissipation rate, while the other inlet boundary conditions have been taken from the referent measurements.

These investigations are expected to be a good start for development of detailed and reliable mathematical model of a two-phase round free jet.

Acknowledgements

This work has been supported by the Republic of Serbia Ministry of Science and Environmental Protection.

References

[1] J.S. Shuen, A.S.P. Solomon, Q.F. Zhang, et al., A theoretical and experimental study of turbulent particle laden jets, NASA CR-168293, 1983.
[2] G.M. Faeth, Recent advances in modelling particle transport properties and dispersion in turbulent flow, in: Proceedings of the ASME-JSME Thermal Engineering Conference, vol. 2, ASME, New York, 1983, pp. 517–534.
[3] C.-P. Mao, G.A. Szekely Jr., G.M. Faeth, Evaluation of a locally homogeneous flow model of spray combustion, J. Energy 4 (1980) 78–87.
[4] J.S. Shuen, A.S.P. Solomon, Q.F. Zhang, et al., The structure of particle-laden jets and non-evaporating sprays, NASA CR-168059, 1983.
[5] G.M. Faeth, Evaporation and combustion of sprays, Prog. Energy Combust. Sci. 9 (1983) 1–76.
[6] S. Yuu, N. Yasukouchi, Y. Hirosawa, et al., Particle turbulent diffusion in a dust laden round jet, AICHE J. 24 (3) (1978) 509–519.
[7] A.D. Gosman, E. Ioannides, Aspects of computer simulation of liquid-fueled combustors, AIAA, 1981 (Paper No. 81-0323).
[8] J.S. Shuen, A.S.P. Solomon, Q.F. Zhang, et al., Structure of particle-laden jets: measurements and predictions, AIAA J. 23 (3) (1985) 396–404.
[9] J. Fan, X. Zhang, L. Chen, et al., New stochastic particle dispersion modelling of a turbulent particle-laden round jet, Chem. Eng. J. 66 (1997) 207–215.
[10] B. Guo, D.F. Fletcher, T.A.G. Langrish, Simulation of the agglomeration in a spray using Lagrangian particle tracking, Appl. Math. Model. 28 (2004) 273–290.
[11] T. Uchiyama, M. Naruse, Numerical simulation for gas-particle two-phase free turbulent flow based on vortex in cell method, Powder Technol. 142 (2004) 193–208.
[12] S. Lain, M. Sommerfeld, Turbulence modulation in dispersed two-phase flow laden with solids from a Lagrangian perspective, Int. J. Heat Fluid Flow 24 (2003) 616–625.
[13] S. Lain, R. Aliod, Discussion on second-order dispersed phase Eulerian equations applied to turbulent particle-laden jet flows, Chem. Eng. Sci. 58 (2003) 4527–4535.
[14] Y.C. Guo, C.K. Chan, K.S. Lau, A pure Eulerian model for simulating dilute spray combustion, Fuel 81 (2002) 2131–2144.
[15] D. Eskin, H. Kalman, A simple model of a cylindrical heavily laden gas-particle jet, Chem. Eng. Sci. 57 (2002) 449–455.
[16] S. Yuu, T. Ueno, T. Umekage, Numerical simulation of the high Reynolds number slit nozzle gas-particle jet using subgrid-scale coupling large eddy simulation, Chem. Eng. Sci. 56 (2001) 4293–4307.
[17] B.B. Ilyushin, D.V. Krasinsky, Large eddy simulation of dynamics of the turbulent round jet with imposed inlet fluctuations, in: Y.D. Chashechkin, V.G. Baydulov (Eds.), Selected Papers of International Conference on Fluxes and Structures in Fluids, 2005, Moscow, June 20–23, 2005, Institute for Problems in Mechanics of the Russian Academy of Sciences, Moscow, 2006, pp. 160–165.
[18] Q. Wang, K.D. Squires, O. Simonin, Large eddy simulation of turbulent gas–solid flows in a vertical channel and evaluation of second-order models, Int. J. Heat Fluid Flow 19 (1998) 505–511.
[19] M. Boivin, O. Simonin, K.D. Squires, On the prediction of gas–solid flows with two-way coupling using large eddy simulation, Phy. Fluids 12 (8) (2000) 2080–2090.

[20] M.W. Vance, K.D. Squires, An approach to parallel computing in an Eulerian–Lagrangian two-phase flow model, in: Proceedings of ASME FED, 2002 ASME Fluids Engineering Division Summer Conference, Montreal, Quebec, Canada, July 14–18, 2002, FEDSM2002-31225.
[21] K. Singh, K.D. Squires, O. Simonin, Evaluation using an LES database of constitutive relations for fluid-particle velocity correlations in fully-developed gas-particle channel flows, in: Fifth International Conference on Multiphase Flow, ICMF'04, Yokohama, Japan, May 30–June 4, 2004 (Paper No. 452).
[22] O. Simonin, P. Fevrier, J. Lavieville, On the spatial distribution of heavy-particle velocities in turbulent flow: from continuous field to particulate chaos, J. Turbulence 3 (2002) 040.
[23] S.V. Apte, K. Mahesh, P. Moin, J.C. Oefelein, Large-eddy simulation of swirling particle-laden flows in a coaxial-jet combustor, Int. J. Multiphase Flow 29 (8) (2003) 1311–1331.
[24] A. Kaufmann, O. Simonin, T. Poinsot, Direct numerical simulation of particle-laden homogeneous isotropic turbulent flows using a two-fluid model formulation, in: Fifth International Conference on Multiphase Flow, ICMF'04, Yokohama, Japan, May 30–June 4, 2004 (Paper No. 443).
[25] J. Makgirk, V. Rodi, Raschet trehmernyh turbulentnyh struy, in: Turbulentnye Sdvigovye Techeniya, Masinostroenie, Moskva, 1982.
[26] M. Stakic, G. Zivkovic, M. Sijercic, Numerical analysis of discrete phase influence of gas flow in a two phase turbulent free jet, in: International Mechanical Engineering Congress, ASME Annual Meeting, 1997, Dallas, 16–21 November 1997, pp. 501–506.
[27] B.E. Launder, G.J. Reece, W. Rodi, Progress in the development of a Re-stress turbulence closure, J. Fluid Mech. 68 (3) (1975) 537–566.
[28] J.O. Hinze, Turbulent fluid and particle interaction, Prog. Heat Mass Tran. (6) (1972) 433–452.
[29] W.K. Melville, K.N.C. Bray, A model of two-phase turbulent jet, Int. J. Heat Mass Tran. (22) (1979) 647–656.
[30] S.K. Fruebkabderm, F.H. Johnstone, Deposition of suspended particles from turbulent gas streams, Ind. Eng. Chem. 49 (1957).
[31] M. Sijercic, S. Oka, V. Vujovic, A contribution to the modelling of turbulent axisymmetric jet, in: Proceedings of Twentieth Yugoslav Congress of Theoretical and Applied Mechanics, Kragujevac, 1993, (in Serbian).